Advanced Structural Mechanics 1 (2023) 258-277

Advanced Structural Mechanics

Journal homepage: https://asm.sku.ac.ir

Evaluation of the effects of link beam on eccentrically braced frames under frequency-domain modal analyses

Masoud Mahdavi[a,*]

[a]PhD Student, K. N. Toosi University of Technology, Tehran , Iran
Article received:2024/04/19, Article revised: 2024/04/23, Article accepted: 2024/04/24

ABSTRACT

Eccentric brace is one of the new methods in seismic improvement of the structure. Placing the link beam in different zones of the brace changes the seismic performance of the bracing system. Therefore, in the present paper, using the finite element method (FEM) and ABAQUS software, 3-story steel structures with eccentric braces are modeled. Eccentric braces have horizontal and vertical link beams. Braced structures are investigated by modal analyses in the frequency domain method. Three types of eccentric braces including (a) middle horizontal beam (EBFK), (b) side horizontal beam (EBFD) and vertical beam (EBFV) are modeled. Also, validation of the models is done with the study by Abdul Hamid et al (2022). The results show that the EBFV model, compared to the EBFK and EBFD models, has a better performance in von mises stress and displacement. The EBFV model reduces the von mises stress by 62.25% and 65.41%, respectively as compared to the EBFK and EBFD models. Moreover, the EBFV model reduces the displacement of the structure by 15.33% and 14.64%, respectively as compared to the EBFK and EBFD models. In comparison to the EBFD and EBFV models, the EBFK model reduces the rotation of the structure by 10.17% and 25%, respectively.
Keywords: Steel Structure, Eccentrically Braced Frame, Link Beam, Modal Analysis, 3D Structure.

1. Introduction

Modern braces are practical methods to increase lateral stiffness in the steel structures. Eccentrically braced frames (EBF) have been developed from 1970 to 1980 by Popov ([1]). The EBF system has been developed in 1972 by Fujimoto et al. in Japan ([2]). There are different types of EBF systems according to the placement of the link beam.

Almasabha and Al-Mazaidh [3] could model a simple truss to estimate the shear strength of the short link in the EBF. [3] recommends switching from the current American institute of steel construction (AISC) equation to the specialized training materials (STM) because the STM predictions have statistical metrics that are noticeably better than the AISC equation, with root mean square error and mean absolute percentage error of 0.27 and 18.6%, 0.22

* *Corresponding author at: K. N. Toosi University of Technology, Tehran , Iran*
E-mail address: M.Mahdavi@email.kntu.ac.ir
DOI: 10.22034/asm.2024.14755.1023: https://asm.sku.ac.ir/article_11607.html

and 14.6%, and built-up and rolled W-shape links, respectively. Kalapodis et al. [4] performed the seismic design of the steel moment-resisting frame, EBF and buckling restrained braced frames by the improved direct displacement-based design method. In this study, the proposed method employs deformation-dependent equivalent modal damping ratios and design modal displacements for the first few modes significantly contributing to the response, as functions of target inter-storey drift representing various performance levels. Chalabi et al. [5] developed a nonmodel rapid seismic assessment of EBF systems incorporating masonry infills using the machine learning method. To this purpose, a set of 4 and 8-story archetype EBF structures considering 12 distinct infill properties, a total number of 48 EBF models, was modeled in OPENSEES software. A nonlinear pushover analysis is then conducted to assess the overall impact of infills on 4 and 8-story structures with EBF systems. Fragility curves at three damage states show accurate predictions and effectively reduce vulnerability in infilled 4-story EBFs. Li et al. [6] conducted a seismic demand assessment on EBF systems. To more accurately evaluate seismic demand on members of EBF, a multiscale numerical model is used to simulate EBF for dynamic analysis. Five EBF models are designed for incremental dynamic analyses and 48 EBF models are used for nonlinear time history analyses at design level. The results show that seismic demands on beams and braces are highly related to overstrength of links at the story. Mata et al. [7] evaluated seismic performance of EBF systems with short-links. This study includes the nonlinear static and dynamic analyses, calibration of numerical link models with experimental studies, and over 15000 models analyzed. Results show that higher ductility and deformation are obtained in most archetypes, while models with 8-story exhibit more stiffness and less ductile behavior. Also, the strength capacity and ductility increase with the increase of the seismic zone and soft type of soil. Mortazavi et al. [8] compared the thermal performance of steel moment frames (SMF) and EBF systems. This investigation was done with OPENSEES software and 3-story structure modeling. Results show that the EBF improves the fire performance of the system by extending the time to collapse. Chen et al. [9] developed the D-type of EBF systems. In this study, the stiffness ratio in the EBF system is recommended to be in the range of 0.35-1.5. Un et al. [10] performed seismic performance evaluation of EBF systems by considering the span length, number of story, the link beam length to bay width ratio and column base condition as the variables. The results showed that strength and stiffness degradation increase the link rotation angle as much as 46% when compared to the nondegrading models. Rezaeian et al. [11] did the experimental study of EBF systems with double vertical link beams. This study proposes a new detail of vertical link beams for EBF systems. The study was conducted with two tests of double vertical link beams specimens under quasistatic loading. The results suggest stable and symmetric hysteresis loops, appropriate seismic behavior and adequate ductility as required by design codes compared to single vertical link beams.

Experimental and numerical testing by previous researchers has shown that links that have shear yield (with short links) provide great stability and ductility in resisting seismic loads. However, the possibility of giving an open area in the architecture makes shorter link selection sometimes insufficient. In many papers such as [6–13], the EBF system has been reviewed. However, there are some shortages in these papers, which include the following:

- Conducting common static and dynamic analyses such as time history and not conducting analyses such as modal in structures with EBF system; The present study is done with modal analysis in the frequency domain, which is one of the innovations of this study.
- Conducting papers with FE modeling of steel frames; Research studies should be done on three-dimensional structures so that the studies are accurate and the results correspond to reality. In the present study, structures are modeled in three-dimensional space and with real length, and the results are completely consistent with real conditions.
- Lack of comparisons between EBF systems with different types of link beams such as horizontal (in the middle and on the sides of the horizontal beam) and vertical; In the present study, all three different states are included in the modeling and the results are practical.
- Placing a short link beam in the EBF system causes disturbances in the architectural space. Therefore, the structure designer should increase the dimension of the link beam. This reduces the stiffness and stability in the EBF system. Therefore, determining the location of the link beam in the EBF system is important and practical. As shown in Fig. 1, in the present paper, three different and new types of link beam in the EBF system are investigated. In general, attempt are made in the present study to fully investigate the existing and expressed deficiencies in order to create appropriate and practical results.

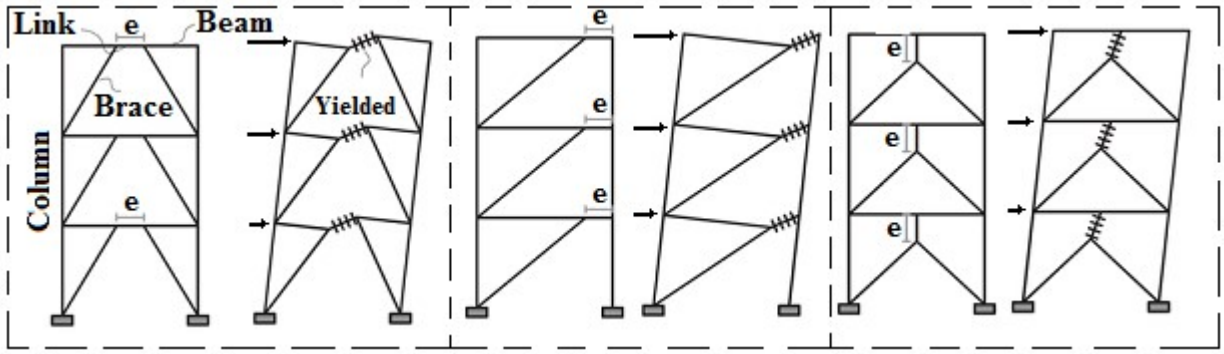

(a) (b) (c)

Fig. 1. Types and short names of eccentric braces in the present paper (a) EBFK; (b) EBFD; (c) EBFV

2. Methodology

2.1. Finite Element Modeling

In the present study, 3-story steel structures (three-dimensional) are modeled with ABAQUS software. The structures are geometrically symmetrical and made of steel with St37 materials. Figure 2 shows the geometry of the modeled buildings in this study. In Fig. 3, the geometric characteristics of the story plan in a 3-story structure are presented. For software modeling, structure elements including column (Three dimensional-solid shape-Extrusion type), beam (Three dimensional-Solid shape-Extrusion type), brace (Three dimensional-Solid shape-Extrusion type) and connection plate (Two dimensional-shell shape-deformable type) are used. After FE modeling, steel sections are assigned to all elements. The elements are then assembled according to the type of brace. In the step module, modal type analysis is selected in the frequency domain. In the present study, three vibration modes in braced frames are investigated. The value of vector using per iteration and maximum number of iteration are taken as 33 and 50, respectively. Considering that the entire braced frame is made of St37 steel, interaction between the members is not considered. The bases of the columns are defined in a steel frame, joined to the ground by fixed supports (Fig. 4). In Fig. 5, the meshing of software elements is presented.

2.2. Modal Analysis in the Frequency Domain

In general, modal analysis in the frequency domain for modal parameters extraction includes natural frequencies, damping coefficients and modal constants. Considering that the experimental data can be in the form of frequency response factor or impulse response factor, different modal analysis methods are developed in the frequency and time domains. In general, the accuracy of modal analysis does not depend on the quality of frequency curve optimization. Increasing accuracy in frequency responses increases accuracy in optimizing the performance curve. By defining a suitable and complete mathematical model, much better results are achieved in frequency response. Therefore, the accuracy of the results will increase [14]. In general, if damping in the system with one degree of freedom is represented by damping matrix, the motion equation is as follows (Equation 1):

$$[M]\{\ddot{x}\}+[C]\{\dot{x}\}+[K]\{x\}=\{0\} \quad (1)$$

Where:

M: The mass matrix,
C: The damping matrix,
K: The stiffness matrix,
x: The displacement vector,
$\dot{x}$: The velocity vector,
$\ddot{x}$: The acceleration vector [14].

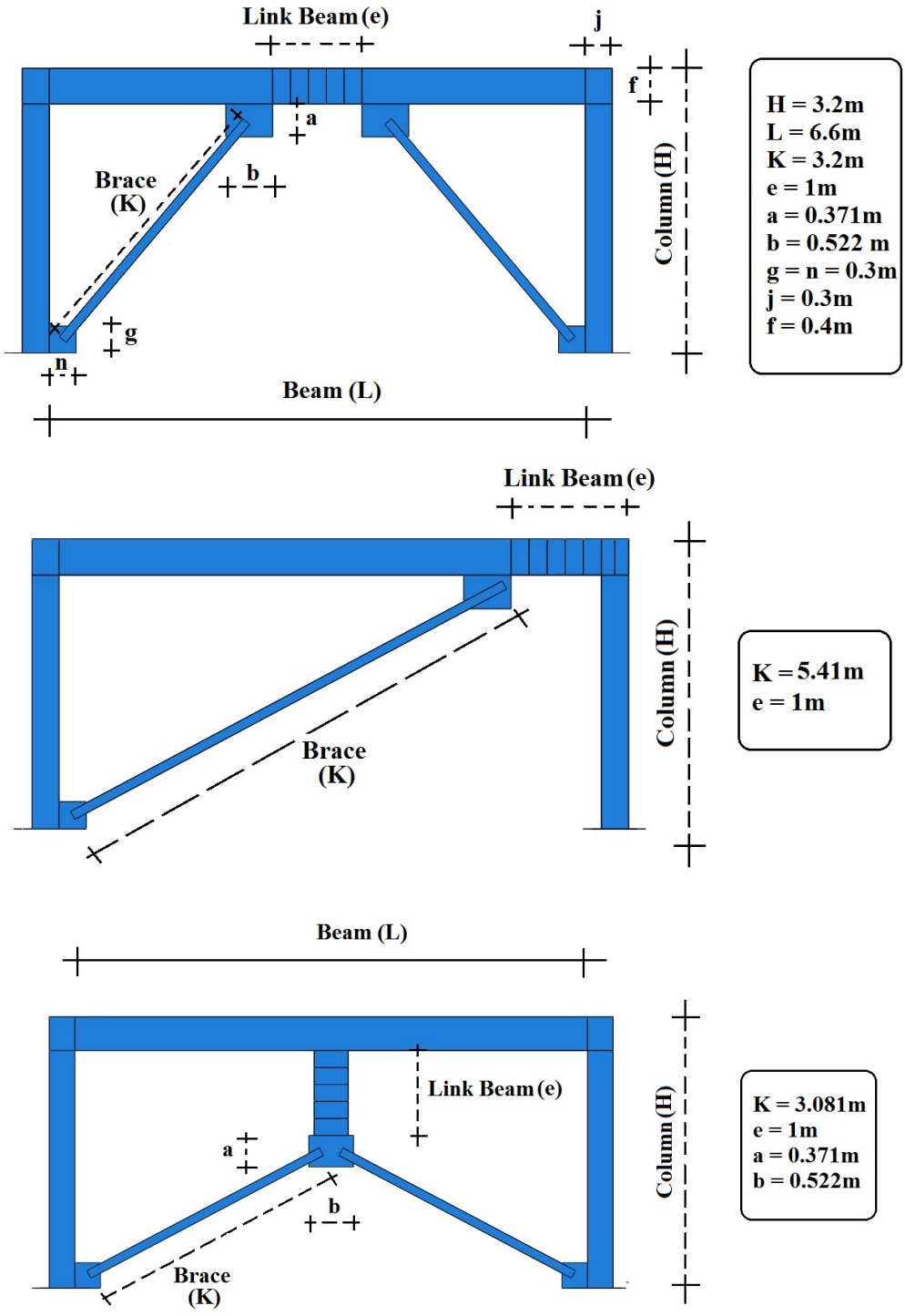

Fig. 2. Geometric dimensions of eccentrically braced frames in the present study

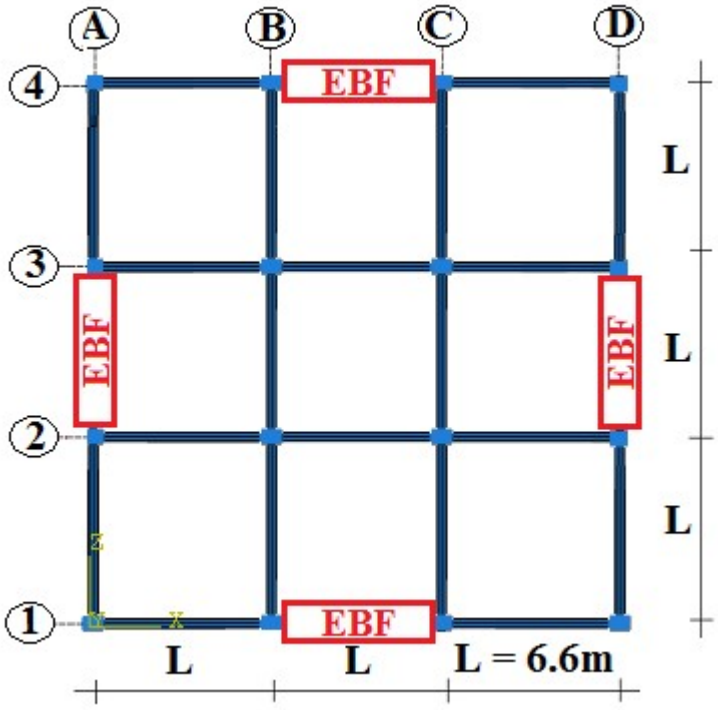

Fig. 3. Story plan in a 3-story structure in the present study

a

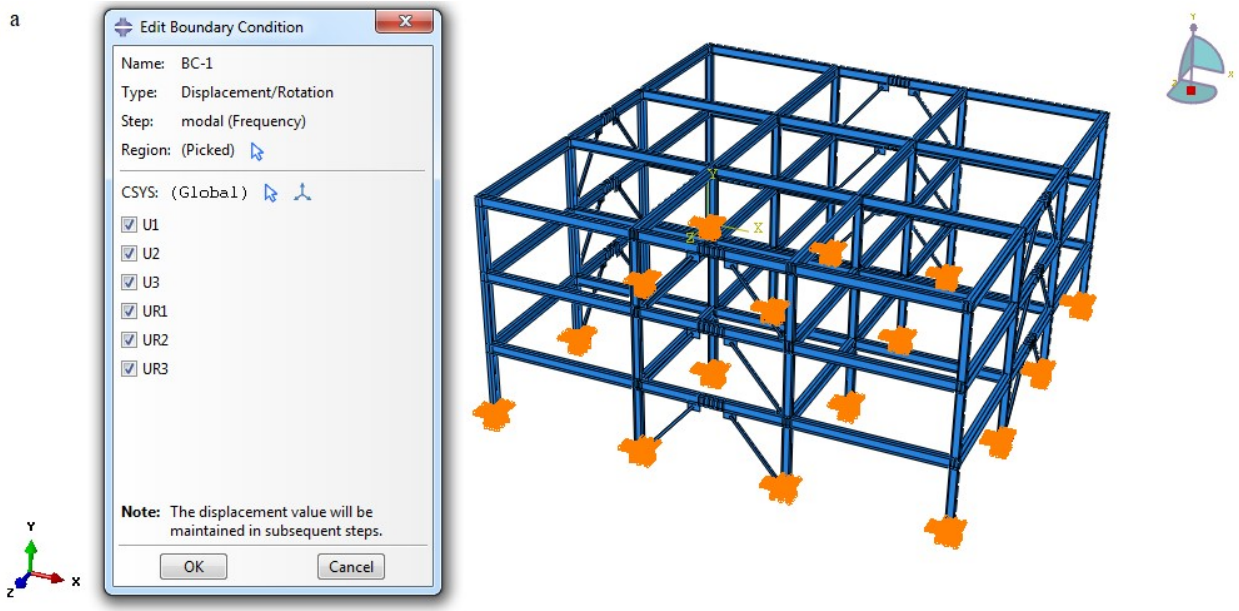

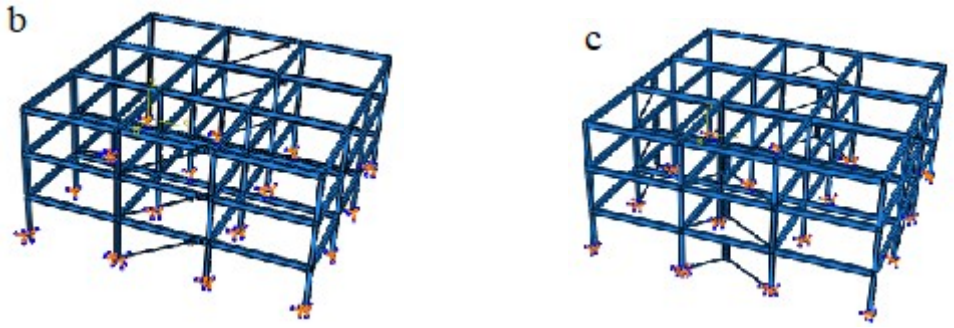

Fig. 4. Steel structures with fixed supports in ABAQUS software (a) EBFK; (b) EBFD; (c) EBFV

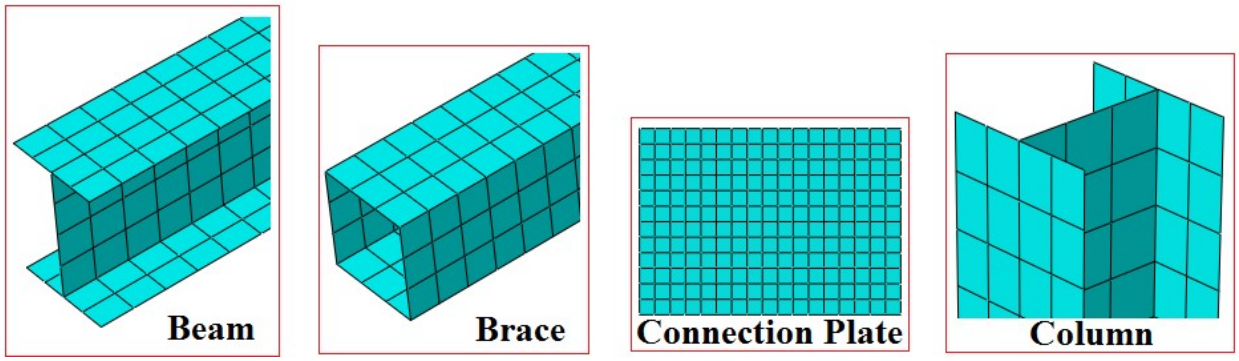

Fig. 5. Elements meshing in software modeling

2.3. Theoretical Topics

2.3.1. Von Mises Stress

Von Mises stress is a value used to determine if a given material will yield or fracture. It is mostly used for ductile materials, such as metals. The von mises yield criterion states that if the von mises stress of a material under load is equal to or greater than the yield limit of the same material under simple tension then the material will yield. It is commonly accepted that the history of elasticity theory began with the studies of Robert Hooke in the 17th century who explored the fundamental concepts of the deformation of a spring and the displacement of a beam. However, engineering wasn't the only reason for the study of elasticity theory, as that research was also linked to an attempt of interpreting nature and the theory of ether. It has been only in the 19th century that the quantitative and mathematical theory of the elasticity of bodies was born, together with continuum mechanics. This allowed the use of integral and differential calculus when modeling elastic phenomena. The continuum mechanics assumes homogenization of the medium, such that microscopic fluctuations are averaged and a continuous field that models the medium can be obtained. Therefore, this implies that for every instant of time and every point in space occupied by the medium, there exists a punctual particle [15–17]. Many theories and concepts stem from the basic concept of continuum mechanics. One of those is the maximum distortion energy theory, which is applied in many fields, such as rubber bearings and applications with other ductile materials. It was Hubert who initially proposed it in 1904, and then von mises developed it further in 1913. According to the maximum distortion energy theory, yielding occurs when the distortion energy reaches a critical value. This critical value, which is material specific, can be easily obtained through a simple tension test [17].

2.3.2. Yielding

When a body, in an initial state of equilibrium or undeformed state, is subjected to a body force or a surface force, the body deforms correspondingly until it reaches a new state of mechanical equilibrium or deformed state. The inner body forces are the result of a force field such as gravity, while the surface forces are those applied on the body through contact with other bodies [18]. The relations among external forces which characterize what is called stress and the deformation of the body, which characterizes strain, are called Stress-Strain relations. These relations represent properties of the material that compose the body and are also known as constitutive equations. Figure 6 explains the curve obtained when studying the strain response of the uniaxial tension of a mild steel beam. These will help us understand why von mises is important. The description of each emphasized point:

- Elastic Limit: The elastic limit defines the region where energy is not lost during the process of stressing and straining. That is, the processes that do not exceed the elastic limit are reversible. This limit is also called yield stress. Above that limit, the deformations stop being elastic and start being plastic; and the deformation includes an irreversible part. The stress value of the elastic limit is used here as S_y [19].
- Upper yield and lower yield: When mild steel is in the plastic range and reaches a critical point called the upper yield limit, it will drop quickly to the lower yield limit, from which deformation happens at constant stress until it starts resisting deformation again [19].
- Rupture stress: Rupture, or fracture, is the separation of an object caused by stress. Therefore, at this point, a fracture of the body is expected. Materials such as mild steel which have the property of fracturing only after large plastic deformations are called ductile. The fracture illustrated here is called a ductile fracture. You can recognize a ductile fracture when the diagram has a curve like the one shown below. This means that as the material gets thinner, more pressure is applied until it suddenly breaks at the rupture stress point [18,19].

2.3.3. Von Mises Yield Criterion

The von mises stress is a criterion for yielding widely used for metals and other ductile materials. It states that a body will yield if the stress components acting on it are greater than this threshold.

$$k^2 = \frac{1}{6}\left[\left(\tau_{11}-\tau_{22}\right)^2+\left(\tau_{22}-\tau_{33}\right)^2+\left(\tau_{33}-\tau_{11}\right)^2+6\left(\tau_{12}^2+\tau_{23}^2+\tau_{13}^2\right)\right] \tag{1}$$

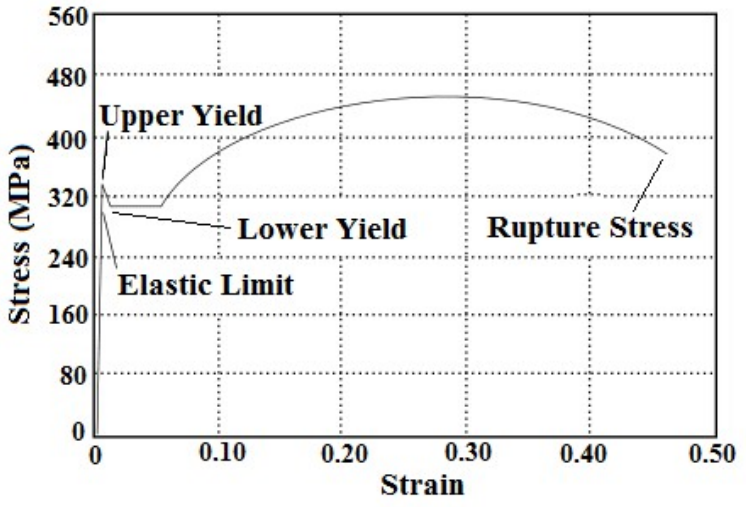

Fig. 6. Stress-strain diagram of St37 steel showing critical stages when under uniaxial force [19]

Where:
k : The constant is defined through experiment,
τ : The stress tensor [19]. Common experiments for defining k are made from uniaxial stress, where the above expression reduces to:

$$\frac{\tau_y^2}{3} = k^2 \tag{2}$$

Where:
τ_y : The simple tension elastic limit. If τ_y reaches the simple tension elastic limit, S_y then:

$$\frac{S_y^2}{3} = k^2 \tag{3}$$

That can be substituted into the Equation (1):

$$\frac{S_y^2}{3} = \frac{1}{6}\left[\left(\tau_{11}-\tau_{22}\right)^2+\left(\tau_{22}-\tau_{33}\right)^2+\left(\tau_{33}-\tau_{11}\right)^2+6\left(\tau_{12}^2+\tau_{23}^2+\tau_{13}^2\right)\right] \tag{4}$$

Or, finally:

$$S_y = \sqrt{\frac{\left[\left(\tau_{11}-\tau_{22}\right)^2+\left(\tau_{22}-\tau_{33}\right)^2+\left(\tau_{33}-\tau_{11}\right)^2+6\left(\tau_{12}^2+\tau_{23}^2+\tau_{13}^2\right)\right]}{2}} \tag{5}$$

The von mises stress (τ_ν) is defined as:

$$\tau_\nu{}^2 = 3k^2 \tag{6}$$

Therefore, the von mises yield criterion is also commonly rewritten as:

$$\tau_\nu \geq S_y \tag{7}$$

That is, if the von mises stress is greater than the tension yield limit stress, then the material is expected to yield. The von mises stress is not real. It is a theoretical value that allows the comparison between the general tridimensional stress with the uniaxial stress yield limit [19]. The von mises yield criterion is also known as the octahedral yield criterion. This is due to the fact that the shearing stress acting on the octahedral planes:

$$\tau_{oct} = \frac{1}{3}\sqrt{\left(\tau_1-\tau_2\right)^2+\left(\tau_2-\tau_3\right)^2+\left(\tau_3-\tau_1\right)^2} \tag{8}$$

and, by applying this result in the octahedral stress expression:

$$S_y = \sqrt{\frac{(\tau_1 - \tau_2)^2 + (\tau_2 - \tau_3)^2 + (\tau_3 - \tau_1)^2}{2}} \tag{9}$$

Similar to the result obtained for the von mises stress, this defines a criterion based on the octahedral stress. Consequently, if the octahedral stress is greater than the simple stress yield limit, then yield is expected to occur [18,19].

3. Results

3.1. VERIFICATION

Validation of the models in the present study is done using the study by Abdelhamid et al. [20]. Reference [20] focused on the lateral reliability of both systems under seismic loading. Nonlinear static pushover and incremental dynamic analysis (IDA) are performed on 5-story and 10-story K and Y-shaped EBFs. A series of 14 near-field and 7 far-field seismic records are considered to analyze and compare the inter-story drifts of both systems using the Seismostruct software. Moreover, Peak Ground Accelerations (PGA) and the different performance levels are also examined. In Fig. 7, the model examined in [20] and the FE model for validation in the current study are presented. After applying a concentrated load in X and Y directions on the steel frame, the pushover diagram (displacement-base shear) was determined as shown in Fig. 8. The results show that the error is 4.5%, which is acceptable and therefore the modeling in the present study is confirmed.

3.2. Von Mises Stress

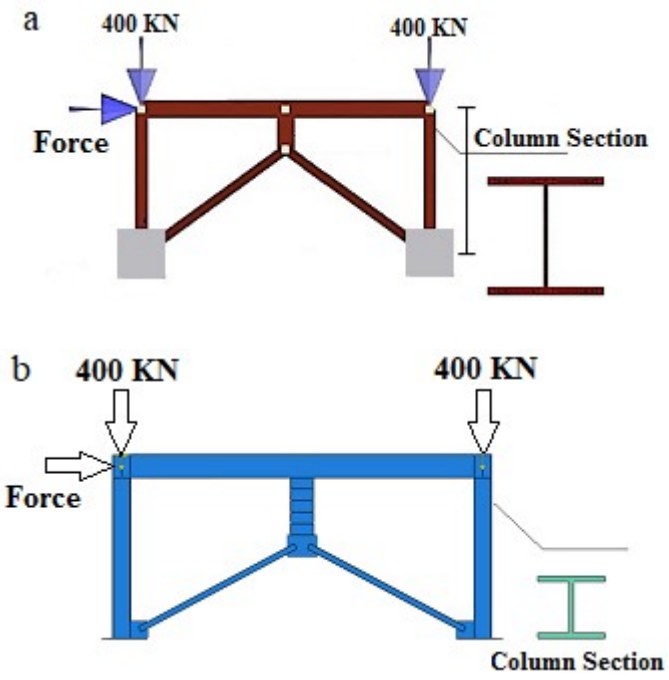

Fig. 7. FE models (a) in [20]; (b) in the present paper.

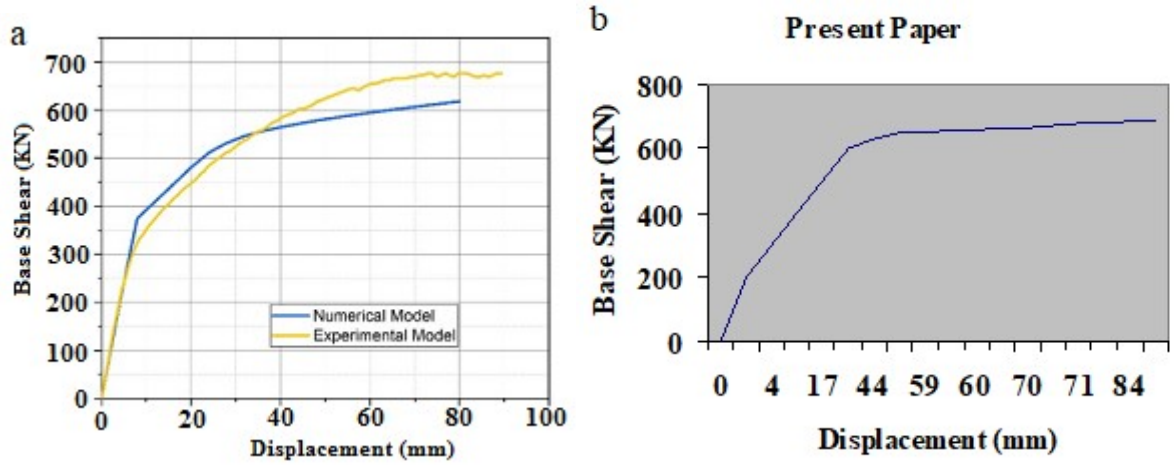

Fig. 8. Pushover curve (a) in [20]; (b) In the present study

Figure 9 shows that the EBFV model has the lowest von mises stress. The average stress in 24 loading steps is equal to 0.302 MPa. The average von mises stress in EBFK and EBFD models is 0.8 and 0.873 MPa, respectively. With a reduction in the von mises stress in the steel structure, the compressive forces on the members reduce. Therefore, during an earthquake or strong storms, the possibility of damage to the structure is reduced. In the von mises stress parameter, the performance of the EBFV system is better than the EBFK and EBFD systems.

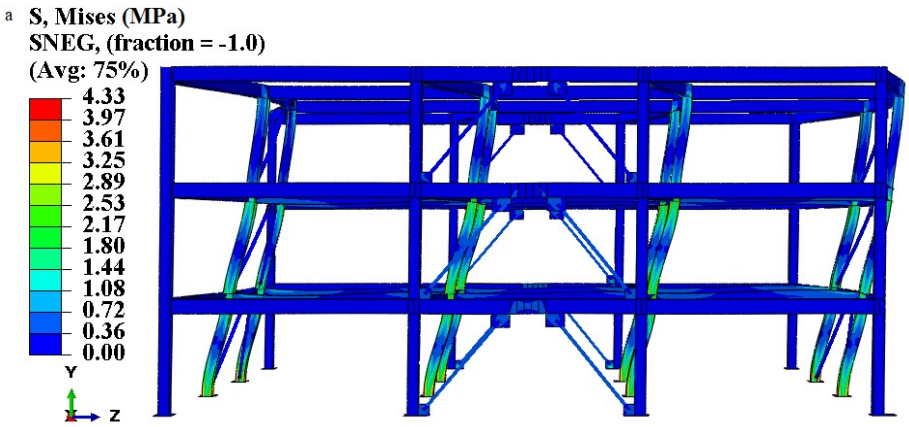

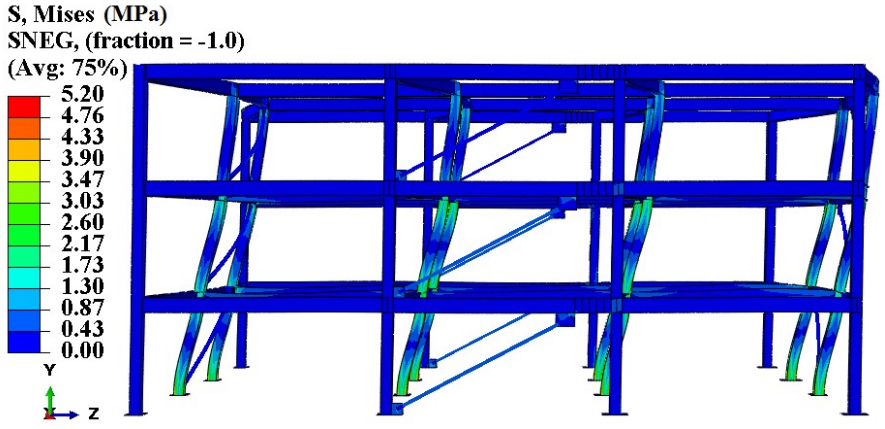
S, Mises (MPa)
SNEG, (fraction = -1.0)
(Avg: 75%)
5.20
4.76
4.33
3.90
3.47
3.03
2.60
2.17
1.73
1.30
0.87
0.43
0.00
Y
Z

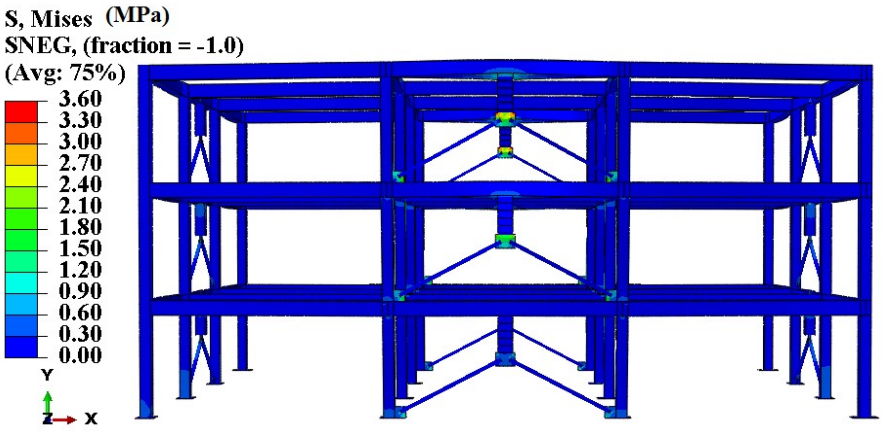
S, Mises (MPa)
SNEG, (fraction = -1.0)
(Avg: 75%)
3.60
3.30
3.00
2.70
2.40
2.10
1.80
1.50
1.20
0.90
0.60
0.30
0.00
Y
X

b

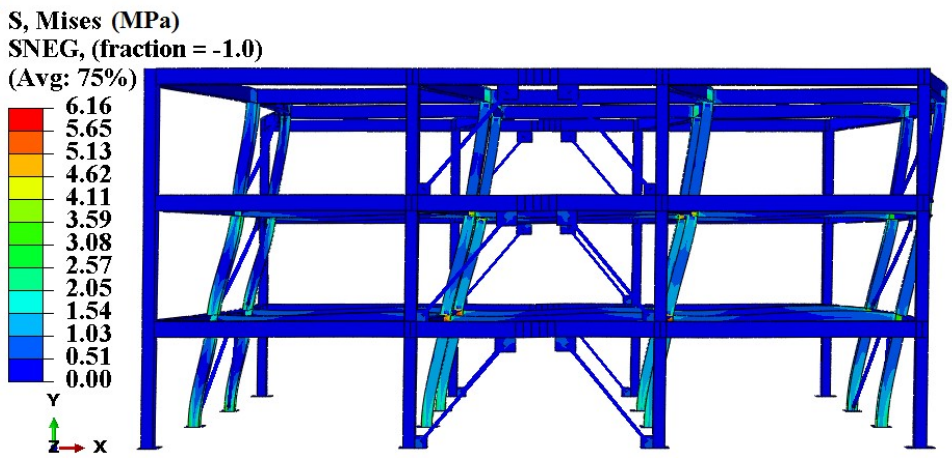
S, Mises (MPa)
SNEG, (fraction = -1.0)
(Avg: 75%)
6.16
5.65
5.13
4.62
4.11
3.59
3.08
2.57
2.05
1.54
1.03
0.51
0.00
Y
X

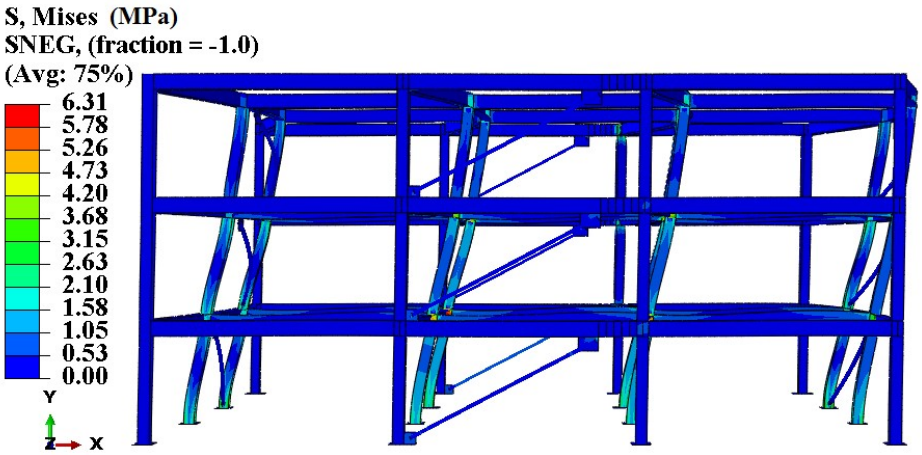
S, Mises (MPa)
SNEG, (fraction = -1.0)
(Avg: 75%)
6.31
5.78
5.26
4.73
4.20
3.68
3.15
2.63
2.10
1.58
1.05
0.53
0.00
Y
Z
X

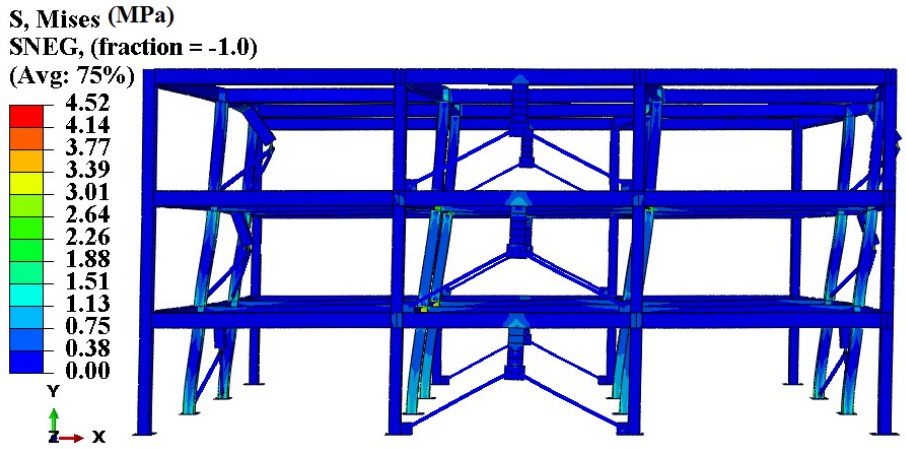
S, Mises (MPa)
SNEG, (fraction = -1.0)
(Avg: 75%)
4.52
4.14
3.77
3.39
3.01
2.64
2.26
1.88
1.51
1.13
0.75
0.38
0.00
Y
Z
X

c

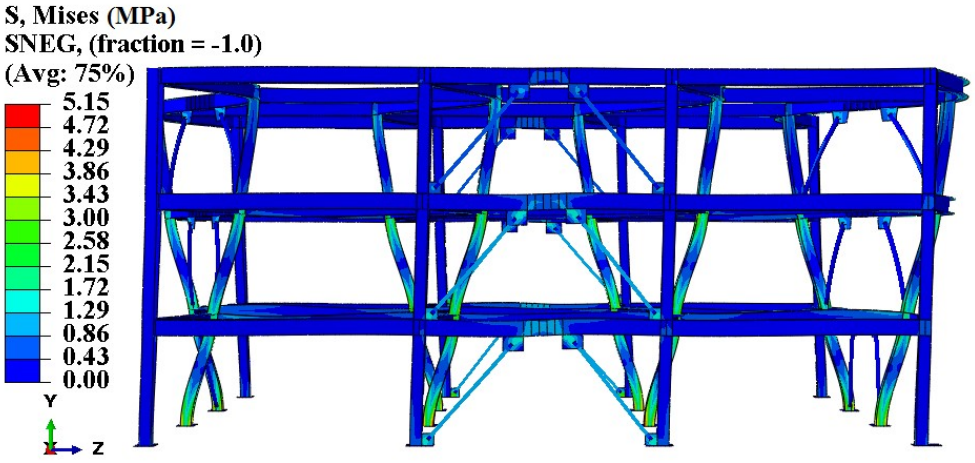
S, Mises (MPa)
SNEG, (fraction = -1.0)
(Avg: 75%)
5.15
4.72
4.29
3.86
3.43
3.00
2.58
2.15
1.72
1.29
0.86
0.43
0.00
Y
Z

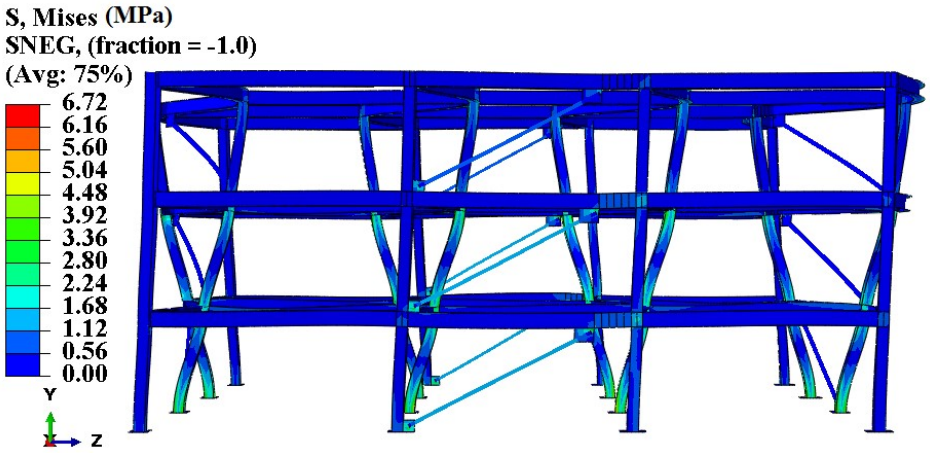
S, Mises (MPa)
SNEG, (fraction = -1.0)
(Avg: 75%)
6.72
6.16
5.60
5.04
4.48
3.92
3.36
2.80
2.24
1.68
1.12
0.56
0.00
Y
Z

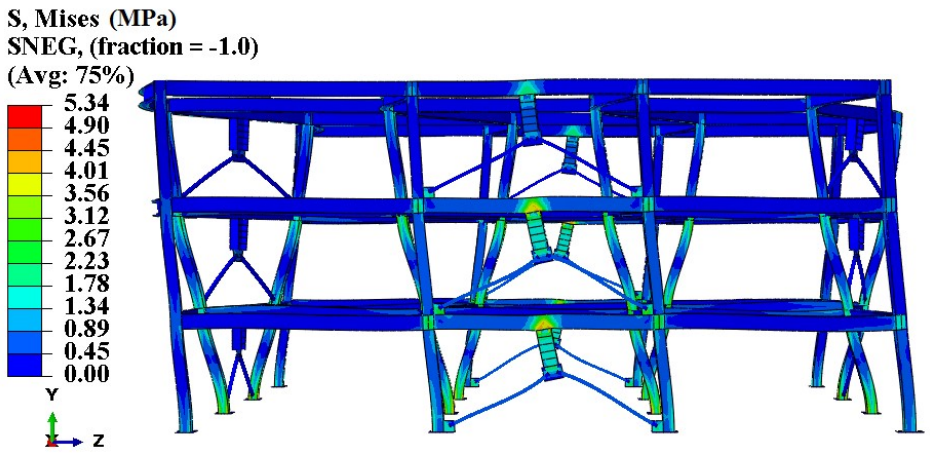
S, Mises (MPa)
SNEG, (fraction = -1.0)
(Avg: 75%)
5.34
4.90
4.45
4.01
3.56
3.12
2.67
2.23
1.78
1.34
0.89
0.45
0.00
Y
Z

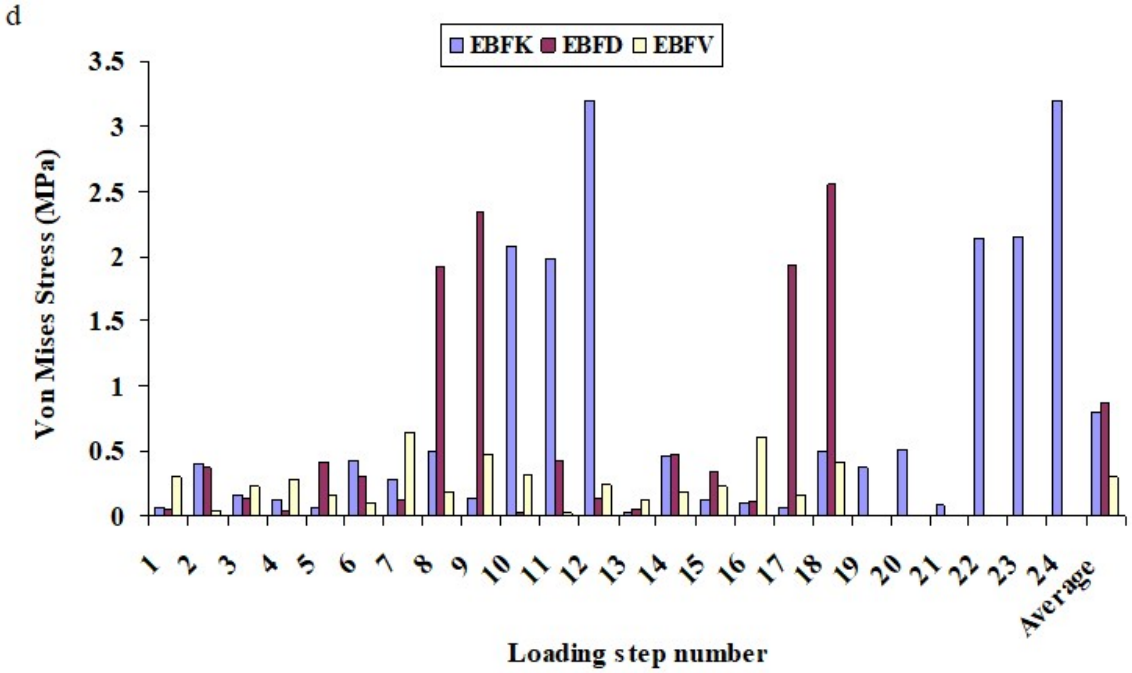

Fig. 9. Von Mises stress (beam-column connection) in 3-story braced structures under modal analyses in the frequency domain (a) EBFK contour; (b) EBFD contour; (c) EBFV contour; (d) Comparison diagram of displacement-mode number.

3.3. Displacement

Figure 10 shows that the EBFV model has the least displacement. The average displacement in three vibration modes for the EBFV model is equal to 0.519 meters. The average displacement in EBFK and EBFD models is 0.613 and 0.608 meters, respectively. The reduction of displacement in the steel structure causes the reduction of the forces (caused by the deviation of the members from the axis) in the structure. As the displacement of the structure increases, greater forces are applied to the members and the probability of damage increases. In the displacement parameter, the performance of the EBFV system is better than the EBFK and EBFD systems.

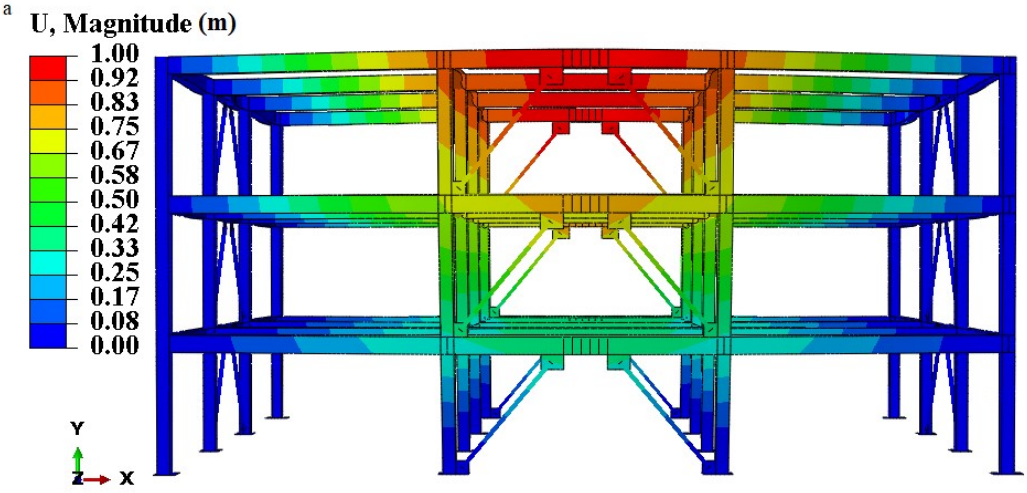

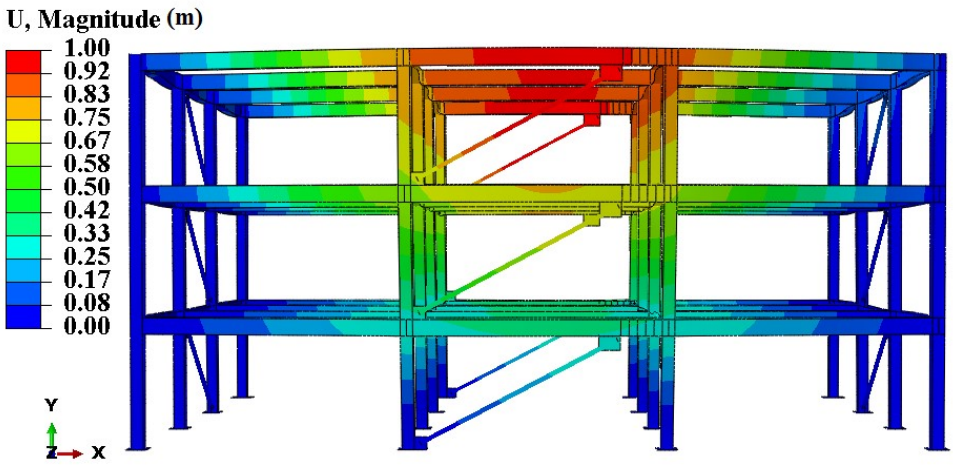
U, Magnitude (m)
1.00
0.92
0.83
0.75
0.67
0.58
0.50
0.42
0.33
0.25
0.17
0.08
0.00
Y
Z
X

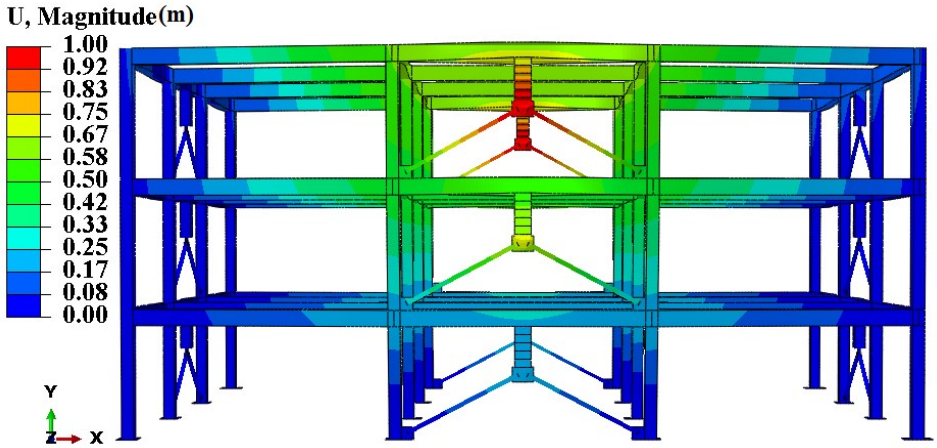
U, Magnitude(m)
1.00
0.92
0.83
0.75
0.67
0.58
0.50
0.42
0.33
0.25
0.17
0.08
0.00
Y
Z
X

b

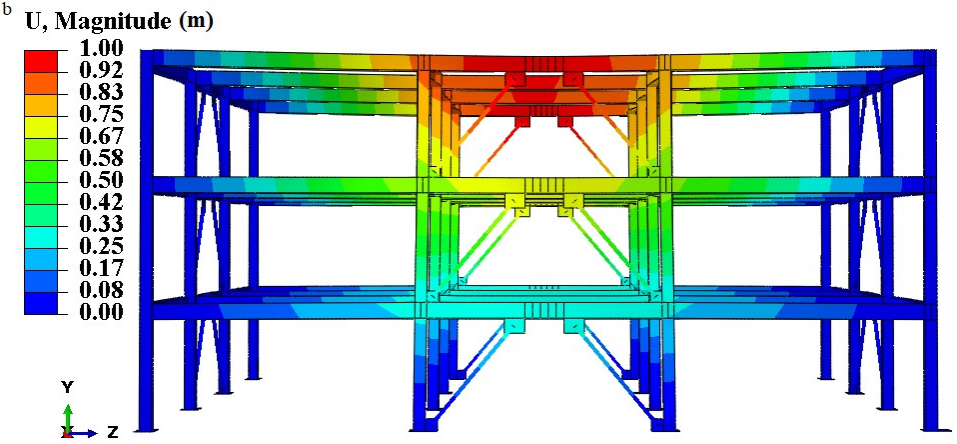
U, Magnitude (m)
1.00
0.92
0.83
0.75
0.67
0.58
0.50
0.42
0.33
0.25
0.17
0.08
0.00
Y
Z

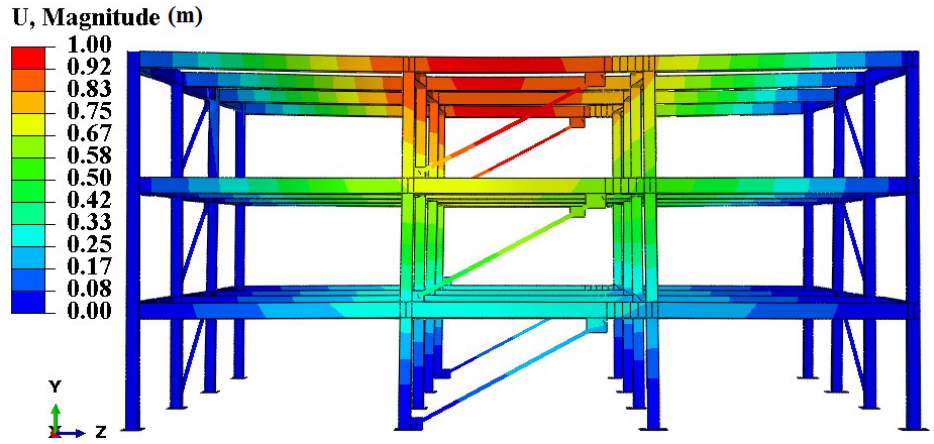
U, Magnitude (m)
1.00
0.92
0.83
0.75
0.67
0.58
0.50
0.42
0.33
0.25
0.17
0.08
0.00
Y
Z

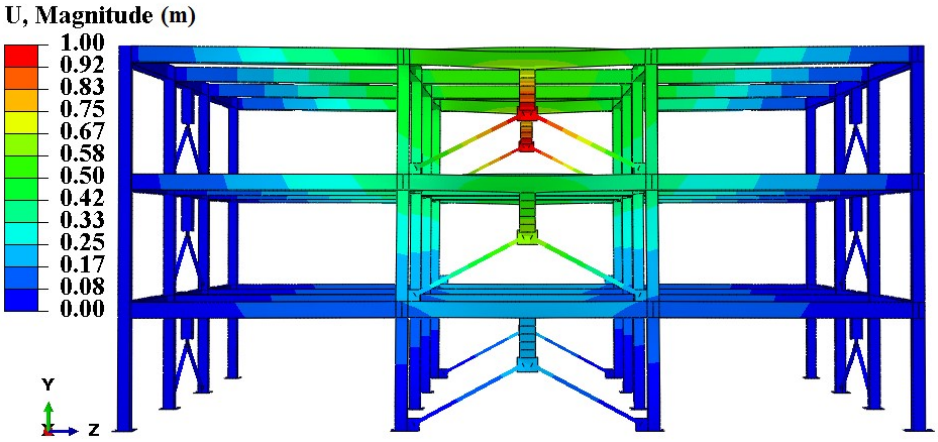
U, Magnitude (m)
1.00
0.92
0.83
0.75
0.67
0.58
0.50
0.42
0.33
0.25
0.17
0.08
0.00
Y
Z

c

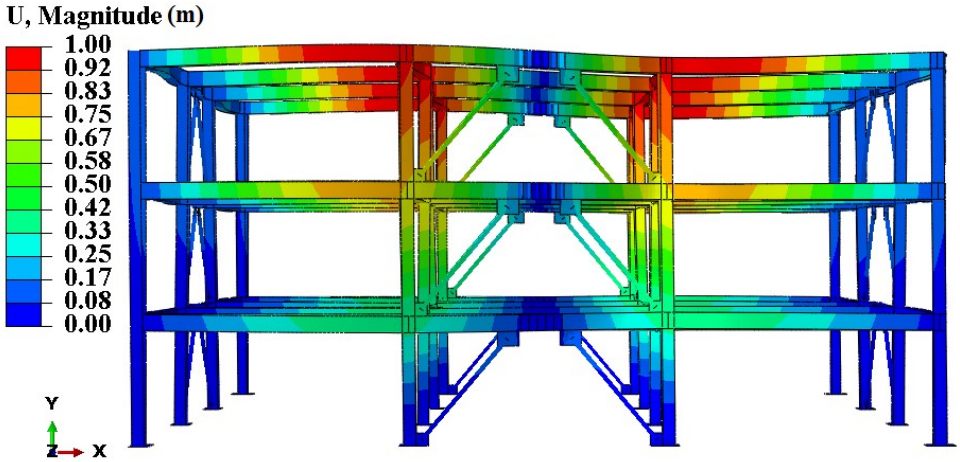
U, Magnitude (m)
1.00
0.92
0.83
0.75
0.67
0.58
0.50
0.42
0.33
0.25
0.17
0.08
0.00
Y
X

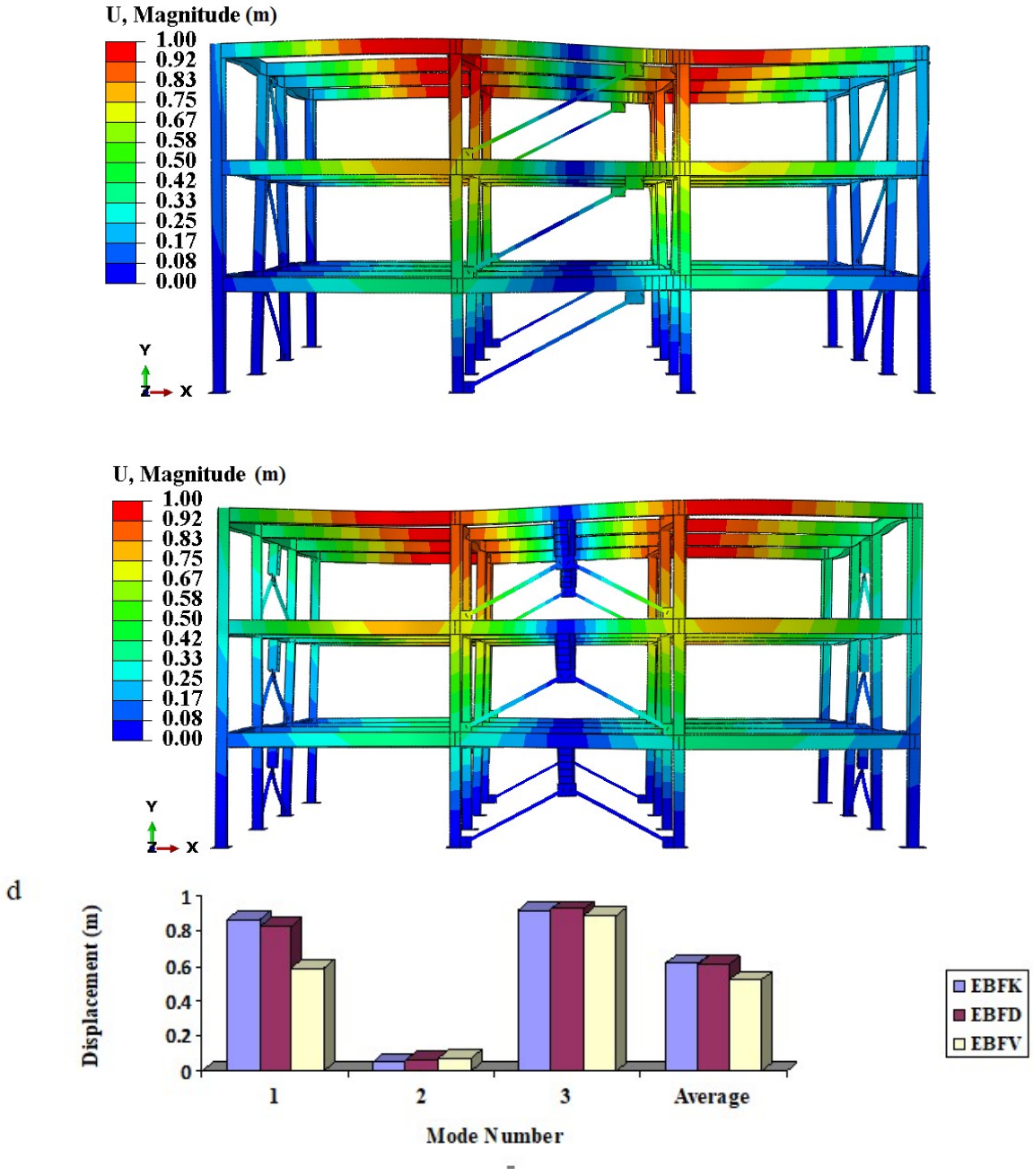

Fig. 10. Mass source displacement in 3-story braced structures under modal analyses in the frequency domain (a) EBFK contour; (b) EBFD contour; (c) EBFV contour; (d) Diagram of displacement-mode number.

3.4. Rotation

Figure 11 shows that the EBFK model has less rotation as compared to the EBFD and EBFV models. It should be noted that in the third mode of the structure, the maximum rotation in the EBFK model is more than the EBFD and EBFV models. But in the first and second modes, the maximum rotation in the EBFK model is less than the EBFD and EBFV models. The total maximum stress during the rotation of the structure (the sum of the first to third modes)

in EBFK, EBFD and EBFV models is equal to 0.000768, 0.000855 and 0.001024 MPa, respectively. By increasing the rotation of the structure during loading, the possibility of damage to the structure, especially the columns, is increased. In general, in the structure rotation parameter, the performance of the EBFK system is better than EBFD and EBFV systems.

Figure 11 shows that the EBFK model has less rotation as compared to the EBFD and EBFV models. It should be noted that in the third mode of the structure, the maximum rotation in the EBFK model is more than the EBFD and EBFV models. But in the first and second modes, the maximum rotation in the EBFK model is less than the EBFD and EBFV models. The total maximum stress during the rotation of the structure (the sum of the first to third modes) in EBFK, EBFD and EBFV models is equal to 0.000768, 0.000855 and 0.001024 MPa, respectively. By increasing the rotation of the structure during loading, the possibility of damage to the structure, especially the columns, is increased. In general, in the structure rotation parameter, the performance of the EBFK system is better than EBFD and EBFV systems.

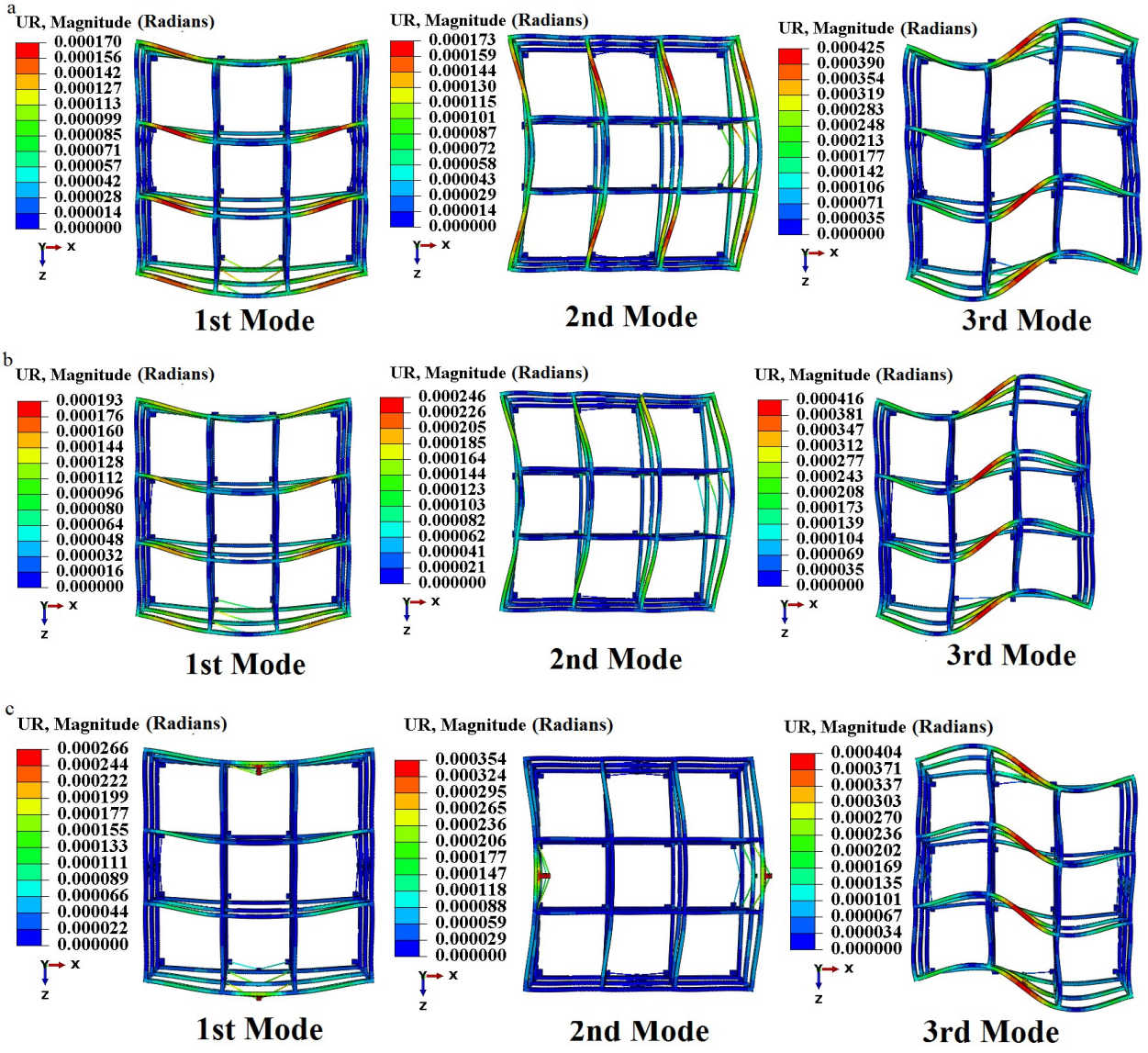

Fig. 11. Rotation in 3-story steel structures under modal analyses in the frequency domain (a) EBFK; (b) EBFD; (c) EBFV

4. Conclusion

In the present study, the performance of 3-story steel structures with eccentric braces and horizontal and vertical link beams is investigated. The horizontal link beams are located in the middle and end of the beam. The vertical link beam is located in the middle of the beam. Modeling is done with FEM and ABAQUS software. The most important results from the present paper are as follows:

- In von mises stress parameter, the model with eccentric brace and vertical link beam (EBFV) has the lowest average stress. The average von mises stress difference in the EBFV model with the EBFK and EBFD models is 62.25% and 65.41%, respectively.
- In the displacement parameter, the model with eccentric brace and vertical link beam (EBFV) has the lowest displacement average. The average displacement difference in the EBFV model with the EBFK and EBFD models is 15.33% and 14.64%, respectively.
- In the rotation parameter, the model with eccentric brace and a central horizontal link beam (EBFK) has the lowest stress resulting from the rotation of the structure. The difference of the total stress resulting from the rotation of the structure in the EBFK model with the EBFD and EBFV models is equal to 10.17% and 25%, respectively.
- The results of the study show that changing the location of the link beam has a great impact on the vibration performance of the braced steel structure, including the rotation of the structure.

References

[1] Mojarad, M., Daei, M., 2023. Effect of brace failure as capacity-based design component on the EBF collapse safety. Structures. 56, e104969.
[2] Yang, T.Y., Neitsch, J., Qissab Al-Janabi, M.A., Tung, D.P., 2020. Seismic performance of eccentrically braced frames designed by the conventional and equivalent energy procedures. Soil Dynamic and Earthquake Engineering. 139, e106322.
[3] Almasabha, G., Al-Mazaidh, R., 2023. Simple Truss Model to estimate the shear strength of short links in the Eccentrically Braced Frame (EBF) steel system. Thin-Walled Structure. 188, e110811.
[4] Kalapodis, N.A., Muho, E.V., Beskos, D.E., 2022. Seismic design of plane steel MRFS, EBFS and BRBFS by improved direct displacement-based design method. Soil Dynamic and Earthquake Engineering. 153, e107111.
[5] Chalabi, R., Yazdanpanah, O., Dolatshahi, K.M., 2023. Nonmodel rapid seismic assessment of eccentrically braced frames incorporating masonry infills using machine learning techniques. Journal of Building Engineering. 79, e107784.
[6] Li, H., Zhang, W., Wei, Q., 2022. Seismic demand assessment on K-configuration eccentrically braced frames. Structures. 45, 1225–1238.
[7] Mata, R., Nunez, E., Calo, B., Herrera, R., 2023. Seismic performance of eccentrically braced frames with short-links: IDA approach using chilean earthquakes. Journal of Building Engineering. 76, e107186.
[8] Mortazavi, S.J., Mansouri, I., Awoyera, P.O., Hu, J.W., 2022. Comparison of thermal performance of steel moment and eccentrically braced frames. Journal of Building Engineering. 49, e104052.
[9] Chen, Z.P., Zhu, S., Yu, H., Wang, B., 2022. Development of novel SMA-based D-type self-centering eccentrically braced frames. Engineering Structure 260, e114228.
[10] Un, E.M., Al-Janabi, M.A.Q., Topkaya, C., 2022. Seismic performance evaluation of eccentrically braced frames with long links using FEMA P695 methodology. Engineering Structure. 258, e114104.
[11] Rezaeian, A.R., Shayanfar, M.A., Jelokhani, P., 2022. The experimental study of eccentrically braced frames with double vertical links. Journal Construction Steel Research. 199, e107587.
[12] Mahdavi, M., Hosseini, S., Babaafjaei, A., 2023. Modeling and Comparison of Plastic Performance in Ten Types of New Steel Braces under Pushover Analysis. Computational Engineering and Physical Modeling. 6, 79–97.
[13] Al-Janabi M.A.Q., Un, E.M., Topkaya, C., 2022. Development of a loading protocol for long links in eccentrically braced frames. Journal of Construction Steel Research. 193, e107278.
[14] Mahdavi M, 2023. Comparing the Performance of Diagonal, A-Chevron, Gate, Knee, Rhombus and X braces with the Finite Element Method. Advanced Structural Mechanics. 1, e11606.
[15] Mahdavi, M., 2020. Evaluation and Comparison of Seismic Performance of Structural Trusses under Cyclic Loading with finite element method. International Journal of Civil and Environmental Engineering. 4, 341–348.
[16] Mahdavi, M., 2020. Assessing the Impact of Underground Cavities on Buildings with Stepped Foundations on sloping lands. International Journal of Civil and Environmental Engineering. 14, 234–238.
[17] Oluwole, L., Emagbetere, E., 2012. Finite Element Analysis of Von-Mises Stress and in-plane displacements In Ellipsoidal and Circular Cylinderical Petroleum Tankers. Engineering. 5, 167–177.
[18] Capecchi, D., Ruta, G., 2016. Strength of materials and theory of elasticity in 19th century Italy. Cham, Switzerland: Springer International Publishing.
[19] Altenbach, H., Armenàkas, A.E., 2006. Book Review: Advanced Mechanics of Materials and Applied Elasticity. ZAMM Zeitschrift fur Angewandte Mathematik und Mechanik. 86, e681.

[20] Abdelhamid, F., Yahiaoui, D., Saadi, M., Lahbari, N., 2022. Lateral reliability assessment of eccentrically Braced Frames including horizontal and vertical links under seismic loading. Engineering, Technology & Applied Science Research. 12, 8278–8283.